Journal of NUCLEAR SCIENCE and TECHNOLOGY, Vol. 48, No. 8, p. 1193–1205 (2011)

ARTICLE

Uncertainties for the Kalimer Sodium Fast Reactor: Void Reactivity Coefficient, k_{eff}, β_{eff}, Depletion and Radiotoxicity

Dimitri ROCHMAN*, Arjan J. KONING and Dirceu F. DA CRUZ

Nuclear Research and Consultancy Group NRG, Westerduinweg 3, P. O. Box 25, 1755 ZG Petten, The Netherlands

(Received September 22, 2010 and accepted in revised form April 18, 2011)

In this paper, we present the effect of nuclear data and its uncertainties on the core design of the KALIMER-600 Sodium Fast Reactor. The void reactivity coefficient, k_{eff}, and β_{eff} are calculated with uncertainties due to the nuclear data of the main components of the reactor: ^{238}U, ^{239,240}Pu, ^{23}Na, ^{56}Fe, and ^{90}Zr. Two methods are used: the "Total Monte Carlo" method involving many identical calculations with different sets of randomized nuclear data, and the perturbation method using MCNP. In a second step, the depletion is calculated together with radiotoxicity components after irradiation. By the Total Monte Carlo method, uncertainties due to nuclear data are propagated to the fuel composition and radiotoxicity curves.

KEYWORDS: nuclear data, uncertainties, Total Monte Carlo, void reactivity coefficient, Sodium Fast Reactor, depletion, irradiation

I. Introduction

The trend in modern reactor physics is that any simulated reactor quantity needs to be accompanied with uncertainties. To obtain a central value is not enough anymore, and safety authorities and funding agencies are becoming more and more aware that a standard deviation must follow a best estimate (see, for instance, Refs. 1) and 2)). At NRG, we perform nuclear simulations with nuclear data uncertainties on a routine basis.

Recently, we have studied in detail the impact of the sodium nuclear data on the void reactivity coefficient for a simplified model of the Kalimer-600 Sodium Fast Reactor.[3] This study, part of a larger project, focused on a single isotope (sodium) for a single quantity (void reactivity coefficient). A new method of uncertainty propagation, so-called "Total Monte Carlo" or TMC, was applied for the first time on a large-scale system and was considered as a proof of principle[4] (previous demonstrations involved simple systems such as criticality-safety benchmarks[5] or fusion benchmarks[6]).

In this paper, the previously used Kalimer-600 Sodium Fast Reactor model and the TMC method are applied to assess the impact of nuclear data uncertainties on many reactor quantities, depletion, and radiotoxicity due to a large number of isotopes (actinides and structural and coolant materials such as Na, Fe, and Zr). The Kalimer-600 Sodium Fast Reactor model and the TMC method are first presented. In the second part of the paper, results are presented for the sodium void reactivity coefficient, k_{eff}, β_{eff}, depletion, and radiotoxicity. Finally, a nonexhaustive list of the advantages and deficiencies of the present study is given, with some suggestions for future possible work.

II. Description of the Kalimer Model

The specifications for the model are based on the general information found in Refs. 7) and 8) completed with data provided by KAERI.[9] For the missing information not provided by KAERI, assumptions based on other references were made. **Table 1** presents the general specifications of the KALIMER-600 model considered in this study.

Different from the original KALIMER-600, the model used here contains one single fuel zone; the original KALIMER contains three fuel zones with a single enrichment fuel but variable cladding thickness (the outer diameter of the fuel rods is fixed). The fuel zone composed of 333 assemblies is surrounded by reflector assemblies, which in our model has been assumed to be composed of 100% steel. The top and bottom axial reflectors have also been considered in this model. The bottom region contains a graphite moderator region, and the top region a layer of Na followed by a gas plenum. The full core model has been developed for the MCNP4C3 Monte Carlo code.[10]

The core loading is such that at the end of each cycle (with a length of 365 EFPD) one-fourth of the core is replaced by fresh fuel. The remaining assemblies are kept at their places and are not shuffled until the end of their life in the core (after 4 cycles). **Figure 1** shows 1/6 of the core, where the different colors represent the 4 different fuel batches and the control and shutdown rod clusters. The core is loaded using a "semi-random" strategy. Since the assemblies are not shuffled, the equilibrium situation consists of four consecutive

*Corresponding author, E-mail: rochman@nrg.eu

© 2011 Atomic Energy Society of Japan, All Rights Reserved.

Table 1 General specifications of the KALIMER-600 model

Thermal power	1523.4 MWth	Number of assemblies	333
Assembly pitch	18.71 cm	Number of fuel batches	4
Core height	94 cm	Coolant inlet temperature	390 degrees
Pin pitch	10.5 mm	Coolant outlet temperature	545 degrees
Fuel pins/assembly	271	Fuel temperature centerline	680 degrees
Pin outer diameter	9.0 mm	Fuel temperature edge	580 degrees
Pin inner diameter	7.56 mm	Fuel slug diameter	6.55 mm
Clad thickness	0.72 mm	Na gap cladding fuel	0.505 mm
Assembly gap	4.0 mm	Assembly width across flats	17.57 cm
Duct thickness	3.7 mm	Moderator material below fuel	graphite
Cladding material	HT-9 alloy	Thickness of moderator	15.0 cm
Drive fuel charge	U-TRU-10% Zr metal alloy	Metal fuel specific density	15.85 g/cm^3
		Fuel smear density	75% TD

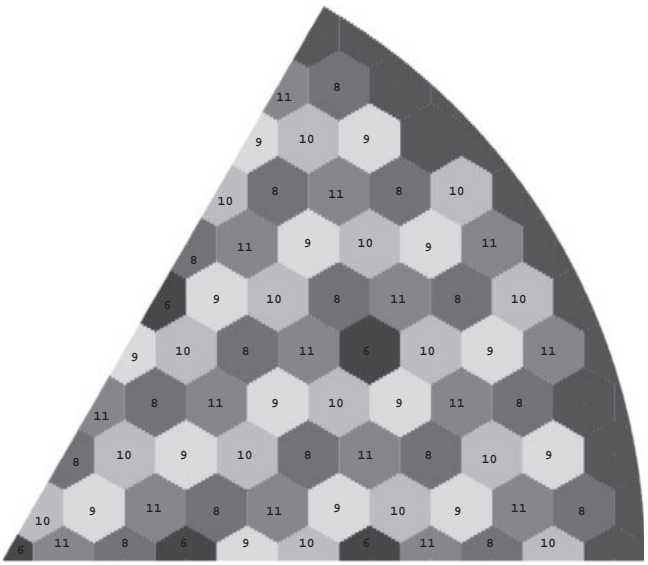

Fig. 1 1/6 full core of KALIMER, where the different colors (labeled 8, 9, 10, and 11) represent the four different fuel batches. The control and shutdown clusters are represented in dark blue (labeled 6).

core configurations. For the calculations described here, the core configuration is taken at the beginning of equilibrium cycle (BOEC). Each of the assemblies is modeled separately, with 271 fuel rods per assembly. No homogenization is applied within the core region.

The fuel is composed of transuranics (TRU) at equilibrium and depleted uranium, in a metallic alloy U-TRU-10% Zr. The TRU composition (presented in **Table 2**) has been provided by KAERI, and calculated under the assumption that the discharged TRU is completely recycled, so that no external feeding of TRU is needed. Only depleted uranium is added to it. Fresh fuel contains 15.5% in volume of TRU (14.6 wt%).

III. Uncertainty Propagation

As of today, two methods can be used at NRG to propagate uncertainties from nuclear data to quantities of large-scale systems. The first one applied in this work is the perturbation method with MCNP, developed at NRG.[11] Both sensitivity profiles and covariance data need to be combined in order to obtain final uncertainties. The second method is the Total Monte Carlo, or TMC (see Refs. 3–5)). This latest method relies on a large number of calculations with the same reactor physics input model, but with unique nuclear data in each of them. The term *nuclear data* includes not only cross sections, but also single and double differential distributions, gamma emission, and nubar (nubar is the average total number of neutrons released per fission event). In short, the complete nuclear data file is unique. The result is a probability distribution from which different moments can be extracted (*i.e.*, average, standard deviation).

Table 2 Isotopic composition of the TRU in the fuel at equilibrium cycle

Isotope	Composition (wt%)	Isotope	Composition (wt%)
^{237}Np	0.437	^{238}Pu	1.392
^{239}Pu	59.485	^{240}Pu	29.102
^{241}Pu	3.069	^{242}Pu	2.533
^{241}Am	2.430	^{242m}Am	0.152
^{243}Am	0.726	^{242}Cm	0.001
^{243}Cm	0.006	^{244}Cm	0.434
^{245}Cm	0.147	^{246}Cm	0.086

The same MCNP model (with MCNP version 4C3[10]) for each of the calculations for the Kalimer model is used in both the TMC and perturbation methods. Likewise, the same version of the processing tools NJOY[12] (version 99.259) and SUSD[13] are used for the entire study. A comparison between both methods is presented in Ref. 14).

The global flowchart of steps for each method is presented in **Fig. 2** in the case of k_{eff} calculations. The nuclear data and their covariances are obtained from the TENDL-2010 library.[15]

1. Perturbation Method

The perturbation approach relies in principle on a unique "NJOY+MCNP+SUSD" calculation. The inputs are the geometry MCNP input file (common to the TMC approach)

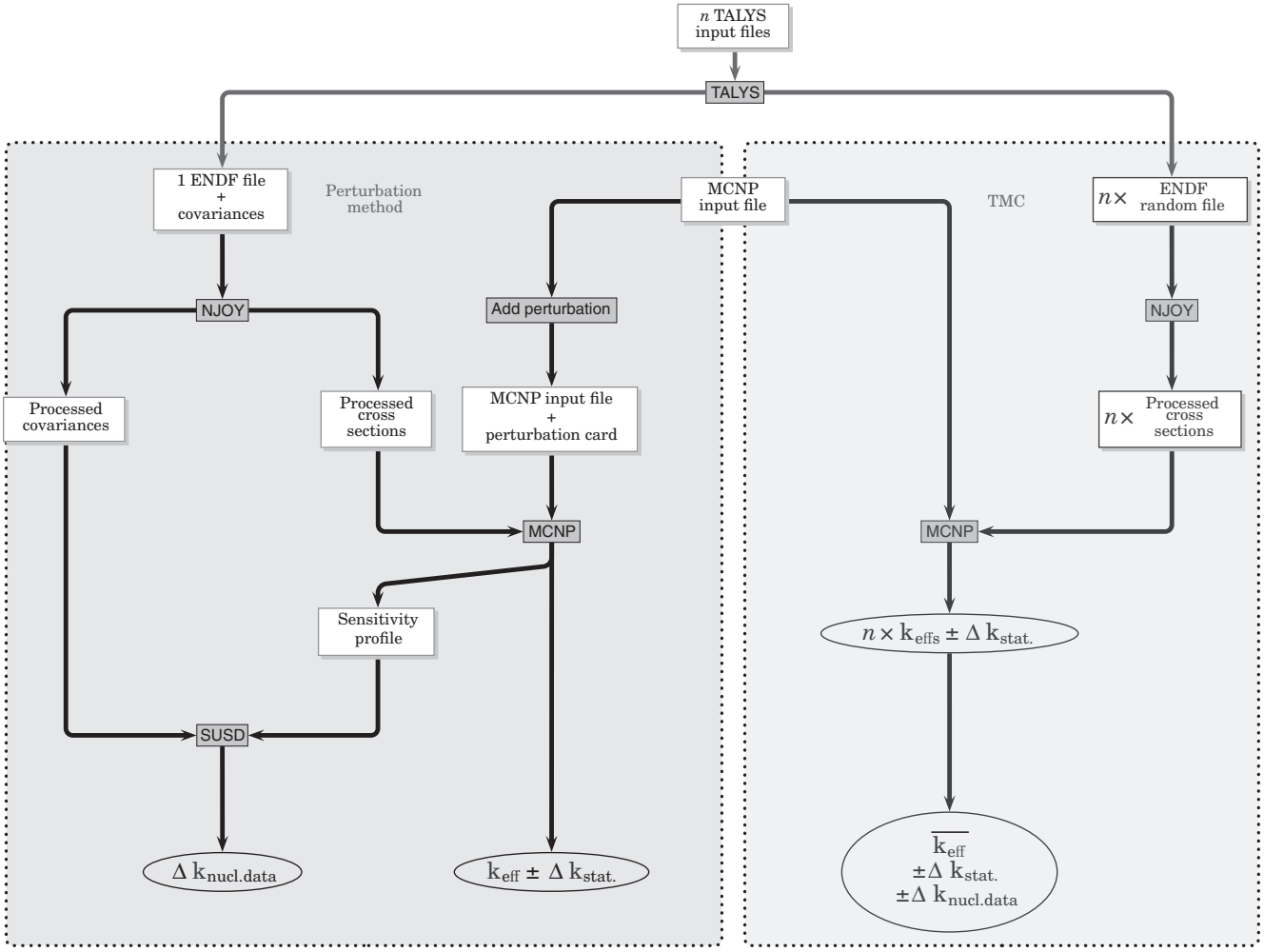

Fig. 2 Flowchart of the uncertainty propagation for TMC and perturbation method

and the ENDF file containing covariances, such as in ENDF/B-VII.0 or TENDL libraries. The sensitivity profile S is defined as the relative change in a response parameter R due to a relative change in cross section in a particular energy group g:

$$S = \frac{(\delta R)/R}{(\delta \sigma_g)/\sigma_g}. \tag{1}$$

In this case, the response parameter is a scalar quantity, which is a function of the incident neutron energy. The sensitivity profile S is obtained using the perturbation option of MCNP, which corresponds to the "PERT"-card:

(1) A cross section is selected for which the profile is to be generated. In the following, four cross sections will be considered: elastic, inelastic, fission, and capture cross sections. Only one specific isotope is varied each time.
(2) A material card is created in which the atomic density for the relevant isotope is increased by 1%.
(3) A "PERT"-card is created specifying that the relevant material is replaced by the perturbed material in each of the cells in which the material is present. Perturbation cards are given for all energy groups. In this paper, the 33-energy group structure (from thermal energy to 20 MeV) is adopted.
(4) Finally, MCNP is run with these modifications in the input. In the MCNP output, a table is given with the results of the perturbations with statistical uncertainties and, in the case of criticality benchmarks, a k_{eff} value with statistical uncertainty.

The processing code NJOY is used in this work to produce nuclear data input files for the MCNP code. These files are usually referred to as ACE files. The sensitivity results and the processed covariances are combined together with the SUSD code. SUSD is a tool for sensitivity-uncertainty analysis. SUSD calculates standard deviations (and sensitivity coefficients) in the design parameters of interest due to input cross sections and their uncertainties. Sensitivity and covariance matrices are produced in a similar energy group. Sensitivities are calculated for cross sections only in the resonance region and fast neutron range. Thus, the effect of angular distribution, double differential data and, in the case of actinides, nubar and fission neutron spectrum, cannot be included in this approach.

2. Total Monte Carlo Method

The Total Monte Carlo method for nuclear data uncertainty propagation was presented in Ref. 4) and extensively applied to criticality-safety benchmarks,[5] the void reactivity

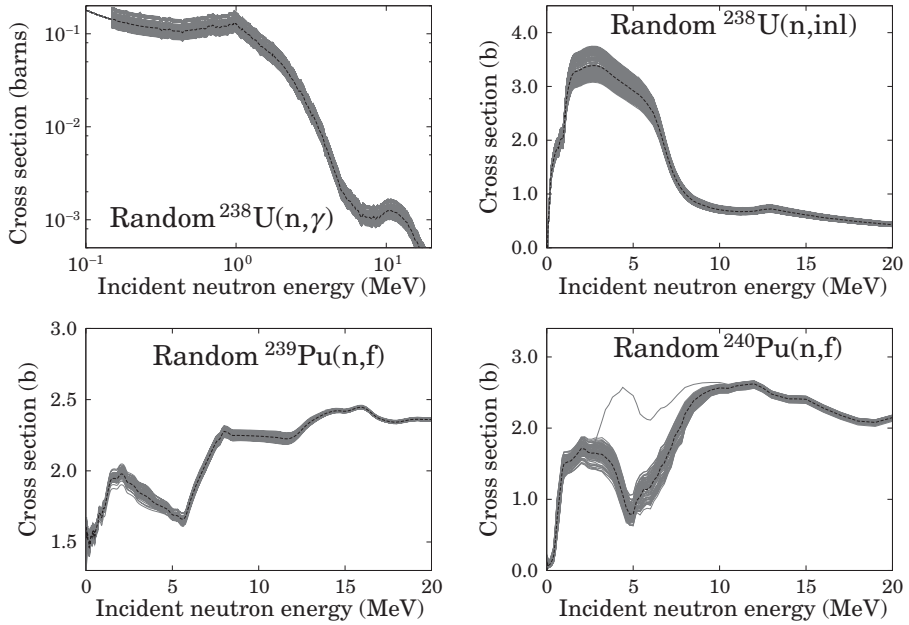

Fig. 3 Central and random cross sections used for the Total Monte Carlo approach for ^{238}U and ^{239,240}Pu. For ^{240}Pu, the outlier is obtained from either statistical effects or computational effects. On the hundreds of cross sections presented in this figure, one is outside the expected uncertainties due to special combinations of model parameters.

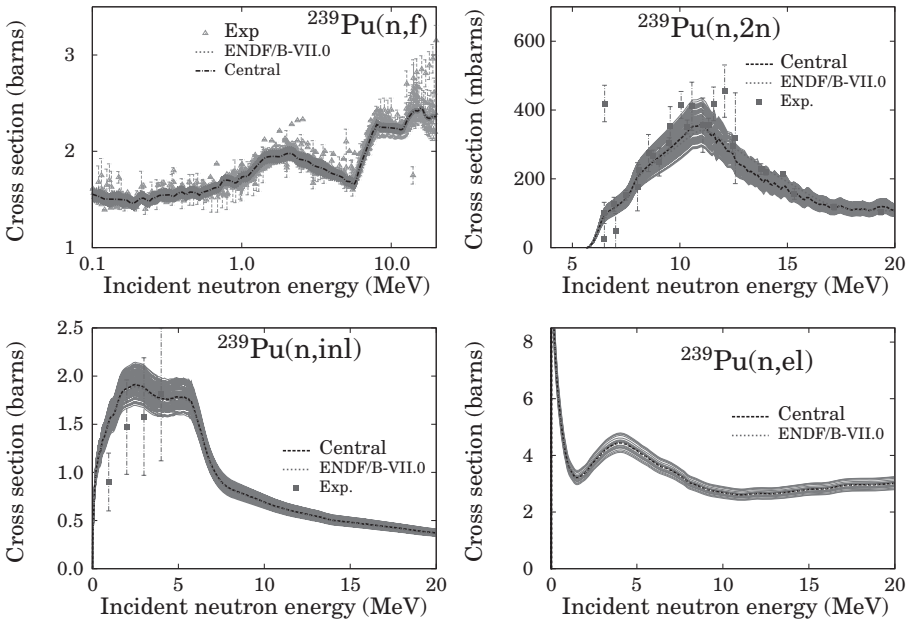

Fig. 4 Central and random cross sections used for the Total Monte Carlo approach for ^{239}Pu compared with experimental data

coefficient of a Sodium Fast Reactor,[3] and fusion benchmarks.[6]

We emphasize again that automation and a disciplined, quality-assured working method (with emphasis on reproducibility) is essential. The input files for this method are an MCNP geometry input file (same as the one used for the perturbation method) and *n* random ENDF files (consistent with the unique ENDF file plus covariances used for the perturbation method). Each random ENDF file is produced using the nuclear reaction code TALYS,[17] is fully reproducible, and consists of a unique set of nuclear data. Each random file is completely different from the next: nubar and energy released per fission ("*MF1 MT456* and *MT458*" in ENDF language), resonance parameters ("*MF2*"), cross sections ("*MF3, all MTs*"), angular distributions ("*MF4 MT2*"), fission neutron spectrum ("*MF5 MT18*"), and double differential data ("*MF6 all MTs*") are varied. **Figures 3** and **4** present some random cross sections for ^{238}U and ^{239,240}Pu.

For each random ENDF file, processing by NJOY is followed by a benchmark calculation performed with

MCNP. At the end of the n calculations, n different k_{eff} values with their statistical uncertainties are obtained. In the obtained probability distribution of k_{eff}, the standard deviation σ_{total} reflects two different effects:

$$\sigma^2_{\text{total}} = \sigma^2_{\text{statistics}} + \sigma^2_{\text{nuclear data}}. \quad (2)$$

The first one ($\sigma_{\text{statistics}}$) is from the statistical uncertainty derived from the number of histories (neutrons) used in the MCNP calculations. It typically varies as $1/\sqrt{N}$; N, being the number of considered histories, is known in advance and in principle can be minimized by investing enough computer time. The second origin ($\sigma_{\text{nuclear data}}$) lies in the use of different random nuclear data files (ACE files) between calculations. It induces a spread in the distribution of the calculated reactor quantity, which can unequivocally be assigned to the spread of cross sections, angular distributions, and so on. This spread is not known and is to be derived from the present Monte Carlo approach. The quadratic sum of the two distinct spreads is equal to the total observed standard deviation. If the observed spread is of the order of the statistical uncertainty (first effect), only a maximum value can be attributed to the spread due to nuclear data.

As mentioned previously, the TMC method allows us to vary much more information than included in the covariance files used by the perturbation method, which considers only resonance parameters ("*MF2*") and cross section ("*MF3*") covariances. It seems therefore natural to always obtain a larger nuclear data uncertainty from the TMC method than from the perturbation method. In order to disentangle the contribution of each class of reactions (the so-called MF numbers), additional ENDF random files are produced together with the full random ENDF files. In these additional files, only their parts are varied. For instance, *MF2 random files* are created where only resonance parameters are varied and the rest of the file stays constant, *MF3 (all MTs) random files* are created where only cross sections are varied, *MF4 MT2 random files* are created where only angular distributions are varied, *etc.* In this manner, benchmarks can be calculated using these partially randomized files and the contribution of specific quantities can be obtained.

3. Limitations

Even if these two methods can be applied to the present study, some inherent drawbacks limit the current approach:

- Strong correlation of calculated nuclear data covariances
  As a result of the use of the TALYS system and theoretical models, energy-energy correlations for a given cross section are quite strong (without the mathematical inclusion of differential experimental data, energy-energy correlations are above 50%). It affects the results in the sense that, for instance, the capture cross section in the fast range will move up or down from one random evaluation to another, keeping a rigid shape. Even if correlations are not basic physical quantities as cross sections, reflecting only the method used to obtain cross sections, it is generally believed that differential experimental data should be mathematically included in the process, and therefore, correlations will be weaker. As a consequence, the shape of cross sections should become less rigid and the benchmark results could vary more. We are currently studying solutions to that problem, as for instance using the "Unified Monte Carlo" presented in Ref. 20).
- Correlations between isotopes
  The covariance files used in this work do not contain cross correlation between isotopes. This is a common issue in nuclear data evaluation, and it is not restricted to this work. Cross correlations between isotopes come from experimental measurements. When a reaction rate is measured, this is performed together with a standard reaction (often a fission chamber containing ^{238}U). The standard reaction is used to normalize the data of interest and to obtain a convenient unit (such as barns). This manipulation brings a strong correlation between the reaction for the isotope of interest and the standard reaction. Cross correlations between isotopes can also come from similar experimental methods used to obtain a nuclear quantity. This deficiency to disregard them in nuclear data evaluation is important when trying to combine uncertainties due to different isotopes to a single value. To avoid this difficulty, we present separate values for uncertainties on the void reactivity coefficient, k_{eff} or β_{eff}.
- Limits of PERT cards in MCNP
  Even if very useful and novel as an MCNP option, some recent tests using the perturbation card (PERT) have shown some differences between this option and more exact solutions.[21] In this reference, it is shown that "*except for the scattering cross section, the sensitivities for the fuel cross sections are within 4% of the direct values. However, the differences are well outside the reported standard deviations. Sensitivities for the reflector cross sections are within only 13–17% of the direct values*, [...]. *The differences are very far outside the reported standard deviations. Inaccurate MCNP k_{eff} perturbation results for spatially localized perturbations have been seen before, both in sensitivity analysis[22] and in reactivity worth calculations[23] for material mass density perturbations, not reaction cross-section perturbations*." The PERT option should then be used with caution and should be tested with other codes such as TSUNAMI.[24] In this work, the PERT card could not be compared with other codes, but comparisons with sensitivity profiles coming from the TMC method are planned. A second limitation of the PERT card is that only cross sections are considered and not other important nuclear data quantities such as ν-bar or the fission neutron spectra.
- No variations of β_{eff} with the PERT option
  The perturbation option in MCNP allows us to obtain sensitivities to k_{eff} only. In the calculation of the sodium void reactivity coefficient uncertainties with MCNP, β_{eff} is considered constant.

Most of the above drawbacks are related to the perturbation method in MCNP, or find their origins in the nuclear data evaluation procedure, which implies limitations for all methods using nuclear data. The TMC method is nevertheless the most general one and contains the least amount of approximations. In the following, the propagation of nuclear data uncertainties on depletion (fuel inventory) and radiotoxocity cannot be done without the TMC method.

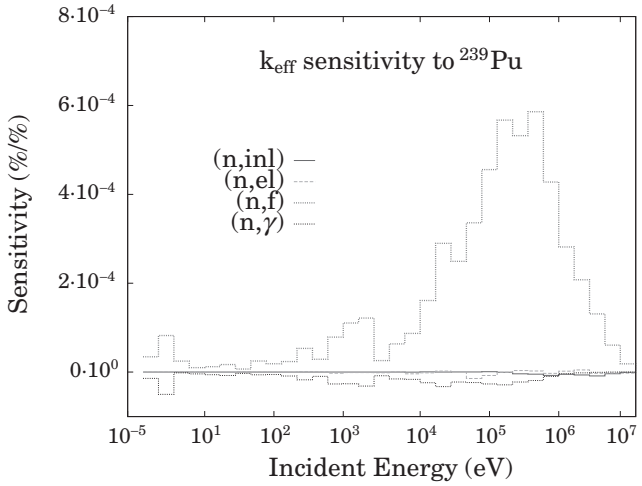

Fig. 5 k_{eff} sensitivity to ^{239}Pu main cross sections for the Kalimer model obtained by the perturbation method

IV. Void Reactivity Coefficient, k_{eff} and β_{eff}

Based on the described methods of uncertainty propagation and the KALIMER model, three reactor quantities were calculated with uncertainty: the sodium void reactivity coefficient, the effective neutron multiplication factor k_{eff}, and the effective delayed neutron fraction β_{eff}. A previous analysis of the required uncertainties[16] indicates that the target accuracy for a typical Sodium Fast Reactor is 3,200 pcm for k_{eff} and 4% for the void reactivity coefficient.

1. Sensitivities

In the present work, sensitivity profiles can only be obtained by the perturbation method. Together with the current approach, we have developed a sensitivity method based on the Monte Carlo evaluations. With the *full* random files, *partial* random files are also being produced: only parts of the evaluation are changed (ν-bar, resonance parameters, or inelastic cross sections...) and the rest of the evaluation is kept unchanged and equal to the evaluation with unperturbed model parameters. By benchmarking these partial random files, sensitivities to ν-bar, cross sections, or fission neutron spectrum can be obtained. Although more exact than traditional sensitivity approaches based on perturbation theories, the principal drawback of this sensitivity method is (for the time being) the needed computational time. This method was successfully applied to the study of a few criticality benchmarks,[18] and we plan to scale up this kind of study for more benchmarks. As an example of sensitivity profiles obtained by the perturbation method, the k_{eff} sensitivities to the main ^{239}Pu cross sections are presented in **Fig. 5** and to other cross sections in **Fig. 6**. As expected, the fission cross section of ^{239}Pu and the capture cross section of ^{238}U have the highest sensitivities (^{239}Pu and ^{238}U are the two main components of the fuel).

The main materials of the Kalimer model are considered in this study, but a few others might as well contribute to the total uncertainties (such as ^{241,242}Pu being more present in mass and with higher nuclear data uncertainties than ^{235}U or ^{238}U). An important quantity not included in the perturbation approach is the uncertainty on ν-bar. Even if well known for Pu and U isotopes, ν-bar has an important impact on k_{eff} and, therefore, on the void reactivity coefficient. To assess the effect of this quantity, the TMC method needs to be applied.

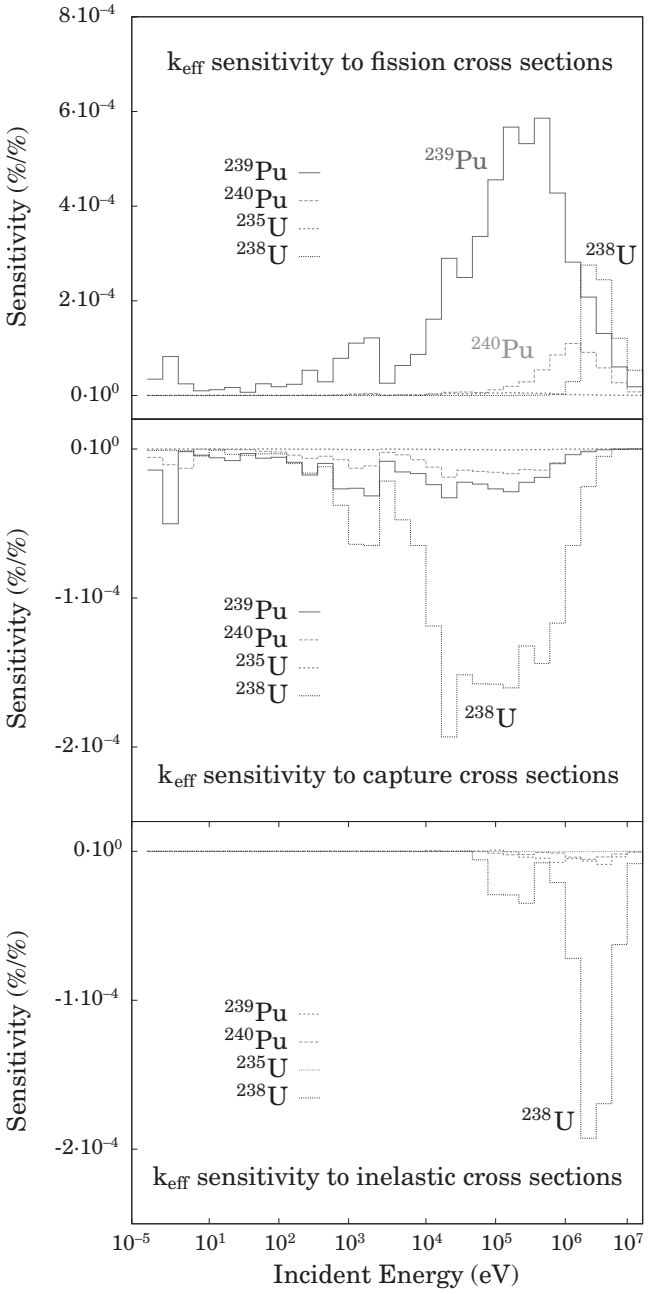

Fig. 6 k_{eff} sensitivity to different cross sections for the Kalimer model obtained by the perturbation method

2. Uncertainties

The perturbation method with MCNP can only be applied to the calculation of k_{eff}. It cannot be used for β_{eff}, but can give a partial answer for the void reactivity coefficient. The sodium void reactivity (SVR) in units of dollars ($) can be obtained with the following equation:

$$SVR = \frac{k_2 - k_1}{k_1 k_2} \frac{1}{\beta_{eff}} \times 10^5, \quad (3)$$

where the number of delayed neutron β_{eff} (in units of pcm) and the k_{eff} values are obtained from the MCNP calculations, following the calculation method presented in Ref. 19). k_1 corresponds to the core flooded with Na coolant, and k_2 to the same core voided of Na coolant. In both cases, the Na coolant present in the axial and radial reflectors is supposed to remain unchanged.

If we suppose that β_{eff} does not vary with different random ENDF files (the beta values and delayed neutron spectra are not randomly changed) and that k_1 and k_2 are fully correlated, the uncertainty on the sodium void reactivity can be expressed as

$$\Delta SVR_{perturbation} = \left| \frac{\Delta k_1}{k_1^2} - \frac{\Delta k_2}{k_2^2} \right| \frac{1}{\beta_{eff}} \times 10^5, \quad (4)$$

with Δk_1 and Δk_2 the uncertainties on k_1 and k_2. In the case of the TMC method, β_{eff} is also varying, which changes Eq. (4). From the composition described in Table 2, the three most important actinides are ^{238}U, ^{239}Pu, and ^{240}Pu. Additionally, coolant and structural materials such as ^{23}Na, ^{56}Fe, and ^{90}Zr are taken into account in this study. Results on the void reactivity coefficient, k_{eff} and β_{eff} are presented in **Tables 3** and **4**.

Figures 7 and **8** show examples of the probability distributions obtained by the TMC method for the void reactivity coefficient and β_{eff}. In the case of the void reactivity coefficient, the spread in the calculated values mainly comes from nuclear data, and the statistical uncertainty is rather

Table 3 Uncertainties on the sodium void reactivity coefficient (SVR) due to different nuclear data uncertainties. Both the perturbation method and TMC were used.

Isotope	Varied nuclear data	Uncertainty on SVR	Method
^{23}Na	all	$\simeq 6\%$	TMC
^{238}U	all	$\simeq 6\%$	TMC
^{239}Pu	all	$\simeq 2.5\%$	TMC
^{239}Pu	(n,f)+(n,γ)	$\simeq 2\%$	Pert.
^{90}Zr	(n,inl)+(n,γ)	$< 0.1\%$	Pert.

Table 4 Uncertainties on k_{eff} and β_{eff} due to different nuclear data uncertainties. Both the perturbation method and TMC were used.

Isotope	Varied nucl. data.	Uncertainty on k_{eff} (pcm)	Method	Uncertainty on β_{eff}	Method
^{238}U	(n,γ)+(n,f)	1,100	Pert.	2.5%	TMC
^{239}Pu	all	800	TMC	1.0%	TMC
^{239}Pu	(n,f)	700	Pert.		
^{240}Pu	all	700	TMC	0.8%	TMC
^{240}Pu	(n,f)	600	Pert.		
^{238}U	(n,inl)	300	Pert.		
^{239}Pu	(n,γ)	260	Pert.		
^{23}Na	all	130	TMC	<1.0%	TMC
^{241}Pu	(n,f)	120	Pert.		
^{56}Fe	(n,inl)	100	Pert.		
^{56}Fe	all	110	TMC	<1.0%	TMC

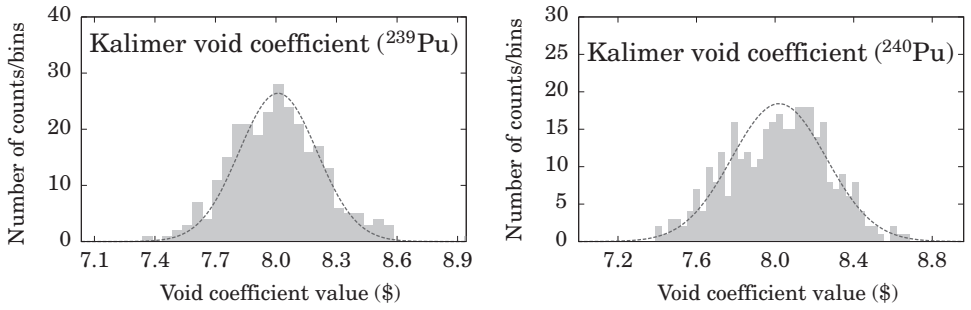

Fig. 7 Calculated sodium void reactivity coefficient (SVR) for the Kalimer-600 design, varying the ^{239,240}Pu nuclear data files

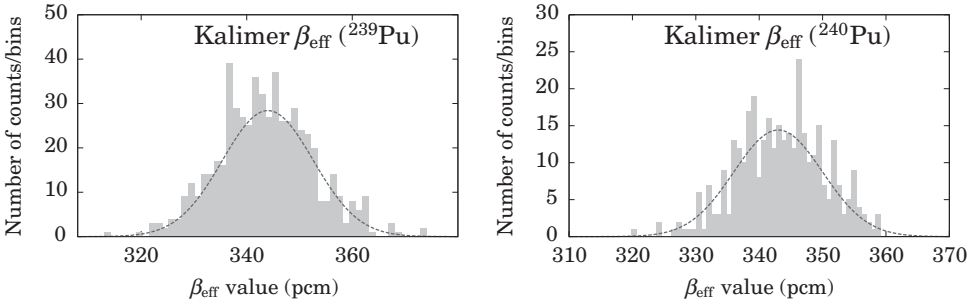

Fig. 8 Calculated β_{eff} for the Kalimer-600 design, varying the ^{239,240}Pu nuclear data files

small (in the order of 1 to 2%). In the case of β_{eff}, as this parameter is not very sensitive to the variation of nuclear data, about half of the spread presented in Fig. 8 is due to statistical uncertainty.

As in the case of the sodium void reactivity coefficient presented in Ref. 3), a normal distribution is obtained for the β_{eff} and k_{eff}. The combination of the two methods allows us to obtain unique results that other approaches cannot provide, such as uncertainties on β_{eff}, or the summed effect of all nuclear data from a single isotope (resonance data, ν-bar, angular distribution, energy spectra): the perturbation method allows us to quickly have an idea of which nuclear data matters, and the TMC method provides more precise results. For the void reactivity coefficient uncertainty as presented in Table 3, this study suggests that the target accuracy of 4% (as presented in Ref. 16)) cannot be met with the actual covariance information.

V. Depletion and Radiotoxicity

Similar to the previous study for the void reactivity coefficient, k_{eff} and β_{eff}, random nuclear data files are used to calculate inventories at the end of the cycle and radiotoxicities up to 10^7 years after irradiation. Each set of random nuclear data files provides a different inventory and radiotoxicity. This is an application of the TMC method to depletion calculations. In the current approach, the random nuclear data files concern the transport part of the calculation and not the activation data used in the inventory code (depletion calculation). This is not a limitation of the TMC method, but rather of the current implementation of the OCTOPUS system (combining MCNP with a depletion code, see below), where the activation files used in the activation code FISPACT cannot easily be changed. It should be kept in mind that the distinction between transport and activation nuclear data is artificial and does not originate from a theoretical background. In principle, if one knows how to generate nuclear data libraries for transport and inventory codes, both transport and activation nuclear data should be changed at once.

There exists only a few methods allowing the assessment of uncertainties due to nuclear data on fuel inventory and the decay of spent fuel after irradiation. An important work is presented in Ref. 25) for an ADS system where the uncertainties due to nuclear data are presented for the inventory at the end of cycle and radiotoxicity curve. Contrary and complementary to the present work, the activation cross section uncertainties were considered and not the transport nuclear data uncertainties. Even if the initial composition of the fuel used in Ref. 25) is richer in minor actinides and that the correlation matrices for cross sections contain very strong correlations (both the fuel composition and the strong correlations tend to increase final uncertainties on depletion and radiotoxicity), the final uncertainties presented in Ref. 25) show that the activation cross sections are a major part of the uncertainty analysis for depletion and radiotoxicity.

1. Depletion Calculations

For the full core depletion simulations, the OCTOPUS modular system[26] has been applied, which permits the link of a 1/2/3-D steady-state neutronics code, such as MCNP or WIMS, to a point depletion code, as ORIGEN or FISPACT, which keeps track of the evolution of the nuclide mixture in the irradiated material, associated with neutron-induced nuclear reactions, such as capture and fission, and decay. The exchange of data between the codes is accomplished by means of the so-called binary interface files. The structure of this code system is flexible enough to allow the coupling of other types of code as well, like uncertainty analysis codes, or codes for the generation of nuclear databases required for full core reactor simulation. In this particular study, MCNP4C3 has been used (as spectrum code) in combination with FISPACT[27] (as the depletion code). For each depletion step, the flux distribution is calculated using MCNP, and in a separate OCTOPUS module, the cross sections for each active isotope (taken from the MCNP point cross section library) are collapsed to few-group cross sections using the spectrum in each depletion zone. For each depletion zone (one separate zone for each of the fuel rods), a separate FISPACT run computes the new isotopic composition using these few-group cross sections.

In the model, 1/6 of the core was considered with reflective boundaries except for the outer radial boundary and the top and bottom surfaces, which are considered as free boundaries (as shown in Fig. 1). Each of the 63 assemblies contained in the 60° angular section is modeled separately and is represented by 6 depletion zones (6 axial nodes). Within each of the six nodes, the 271 fuel rods are modeled separately, however, with a common nuclide inventory. Therefore, a total of 378 depletion zones are considered. The flux to be used by FISPACT is calculated before each depletion step from the total power per assembly, isotopic composition of each depletion zone, flux distribution, and energy released per fission and capture for each nuclide. The same normalization factor is also applied to scale the flux and reaction rate tallies produced by MCNP.

As mentioned before, a large number of similar calculations are performed, randomly changing each time the transport nuclear data files. An example of calculated inventories for a few actinides as a function of irradiation time is presented in **Fig. 9**. The time for one depletion calculation, and thus, for each random set of nuclear data, is rather long (about 5 days on a single 3 GHz CPU), and a total of 250 depletion calculations were performed. This number is sensibly smaller than in the previous sections, but considering the amount of computational power at our disposal, it gives a reasonably precise estimate of the uncertainties. From previous studies using the TMC method (see Ref. 3) or 6)), we can estimate that the uncertainties are known to be about 10% after 250 samples (from standard statistical theory, where, for a normally distributed variable, the error in estimating the variance is $1/\sqrt{N}$).

Table 5 presents the inventory and uncertainties at the end of cycle for important actinides. These uncertainties were obtained by varying the nuclear data for all the actinides presented in Table 5 at once, except for ^{242m}Am, where no random nuclear data were available. It can be noted that the impact of transport nuclear data is not the

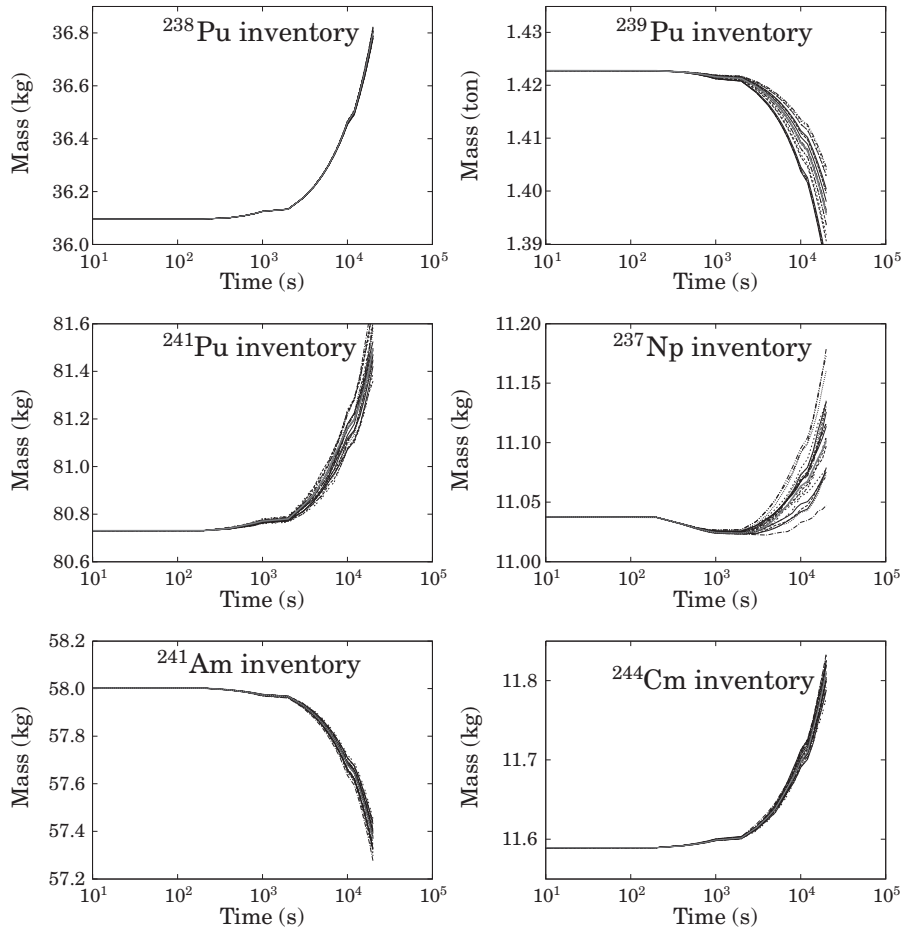

Fig. 9 Examples of calculated inventories for ^{238,239,241}Pu, ^{237}Np, ^{241}Am, and ^{244}Cm. The spread between the curves is due to variations in ^{238}U nuclear data.

same on all actinides. Globally, the nuclear data uncertainties are larger for small quantities of specific actinides.

Two uncertainties are given for each isotope, defining a lower and a higher value. These two values originate from the assumption regarding the correlations between nuclear data. Experimentally, the vast majority of measurements on actinide cross sections is performed relative to a standard, for instance, through a fission chamber for the flux measurements or a normalization factor at a specific energy. In general, depending on the energy range, the standard cross section is the fission cross section of ^{235,238}U, or the capture cross section on ^{197}Au. These experimental normalizations need to be reflected in nuclear data evaluation, because if a standard cross section is later modified, the correlated nuclear data measured relative to the standard have to be changed. This is also the case for the nuclear data covariances, both for covariance files and TMC. If an experimental correlation exists between ^{235}U(n,f) and ^{241}Am(n,f), both cross sections cannot be varied independently. In the case of covariance files, this information is in general not included and it has no effect as long as data users are not using both covariances in the same study. In the case of TMC, a similar problem exists as soon as nuclear data for the standard is varied together with other data. To calculate the total uncertainty for the inventory of a given isotope, the following equations can be used. If Q_{A} is the quantity for the isotope A calculated at the end of cycle, then Q_{A} is a function of all the variables used:

$$Q_{\text{A}} = f(^{238}U, ^{239}Pu, ^{240}Pu \ldots). \tag{5}$$

The resulting uncertainty on Q_{A} is then

$$(\Delta Q_{\text{A}})^2 = \sum_{i=0}^{\text{isotopes}} \left(\frac{\partial f}{\partial x_i} \Delta x_i \right)^2 + 2 \sum_{i \neq j} \frac{\partial f}{\partial x_i} \frac{\partial f}{\partial x_j} \text{corr}(x_i, x_j), \tag{6}$$

where $\text{corr}(x_i, x_j)$ is the correlation term between the two nuclei x_i and x_j (for instance, between ^{238}U and ^{241}Am). In the current use of TMC for depletion and radiotoxicity calculations, the correlation terms are not known (a similar unknown is in general observed with perturbation methods) and the following assumptions can be made:

- Full correlation is assumed, meaning $\text{corr}(x_i, x_j) = 1$. Even if not realistic, this eventuality gives a higher value for the uncertainty on Q_{A}. Equation (6) can be simplified to

$$\Delta Q_{\text{A}} = \sum_{i=0}^{\text{isotopes}} \left| \frac{\partial f}{\partial x_i} \Delta x_i \right|. \tag{7}$$

- No correlation is assumed, meaning $\text{corr}(x_i, x_j) = 0$. Again not realistic, this eventuality gives a lower value for the uncertainty on Q_{A}. Equation (6) can be simplified to

Table 5 Inventory of major and minor actinides at the end of cycle with total uncertainties due to different nuclear data. Some details for different isotope contributions can be found in Table 8. Uncertainties for ^{242m}Am and ^{243}Am are in italic because the nuclear data for ^{242m}Am were not randomized, resulting in a low uncertainty for these two isotopes.

Isotope	Quantity (kg)	Uncertainty (%) Full correlation	Uncertainty (%) No correlation
^{241}Am	57.4	0.4	0.2
^{242}Am	0.00953	10.8	7.4
^{242m}Am	2.8	*0.6*	*0.5*
^{243}Am	18.7	*0.7*	*0.4*
^{244}Am	0.000142	8.4	4.1
^{242}Cm	1.87	7.7	5.4
^{243}Cm	0.18	13.2	12.5
^{244}Cm	11.81	1.0	0.7
^{245}Cm	3.44	8.8	8.6
^{246}Cm	2.18	2.5	2.4
^{237}Np	11.11	1.8	1.2
^{239}Np	0.91	7.4	4.7
^{238}Pu	36.80	0.8	0.7
^{239}Pu	1,396.2	0.5	0.4
^{240}Pu	733.4	0.3	0.2
^{241}Pu	81.5	1.1	0.7
^{242}Pu	64.2	0.5	0.3
^{243}Pu	0.0012	16.0	7.1
^{234}U	1.02	0.3	0.2
^{235}U	17.2	1.0	0.7
^{236}U	1.80	2.1	1.2
^{238}U	11,495.2	0.07	0.04

$$\Delta Q_{\mathrm{A}} = \sqrt{\sum_{i=0}^{\text{isotopes}} \left(\frac{\partial f}{\partial x_i} \Delta x_i \right)^2}. \quad (8)$$

If negative correlations would be considered, an even lower value can be obtained, but negative correlations are restricted to very specific cases and we prefer not to assume a full negative correlation to obtain a lower value for the uncertainty on Q_{A}.

These two limits are presented in Table 5 for the inventory at the end of cycle and for the radiotoxicity (see next section), with more details in **Table 6**.

For major actinides, the uncertainties on the inventory are not important (less than 1%) and might be overcome by the uncertainties due to activation nuclear data. In the case of minor actinides, the impact of transport nuclear data is larger, depending on the quantity present in the irradiated fuel. But generally, the impact of transport nuclear data on the inventory of spent fuel is rather limited. In the case of ^{242m}Am and ^{243}Am, the obtained uncertainties are rather small, due to the fact that the cross sections of ^{242m}Am are kept unchanged.

2. Radiotoxicity

The radiotoxicity of the discharged fuel is calculated in a separate run of FISPACT. As input, the total inventory summed over all the discharged assemblies is provided. The inventory is extracted from the binary interface file

Table 6 Inventory of major and minor actinides at the end of cycle with uncertainties due to different nuclear data (lower limit, with no correlation for the nuclear data)

Isotope	Quantity (kg)	Uncertainty (%) due to ^{238}U	^{239}Pu	^{240}Pu	^{241}Pu	All others	Total (%)
^{241}Am	57.4	0.06	0.07	0.04	0.01	0.21	0.2
^{242}Am	0.00953	1.27	0.92	0.80	0.65	7.16	7.4
^{242m}Am	2.8	0.03	0.06	0.04	0.02	0.44	0.5
^{243}Am	18.7	0.08	0.08	0.06	0.06	0.40	0.4
^{244}Am	0.000142	1.64	1.85	1.08	0.71	3.13	4.1
^{242}Cm	1.87	0.90	0.71	0.65	0.18	5.27	5.4
^{243}Cm	0.18	0.28	0.17	0.20	0.11	12.5	12.5
^{244}Cm	11.81	0.10	0.09	0.06	0.03	0.72	0.7
^{245}Cm	3.44	0.07	0.07	0.06	0.06	8.59	8.6
^{246}Cm	2.18	0.03	0.01	0.01	0.01	2.43	2.4
^{237}Np	11.11	0.29	0.27	0.05	0.08	1.15	1.2
^{239}Np	0.91	4.43	1.26	0.82	0.37	0.54	4.7
^{238}Pu	36.80	0.03	0.02	0.01	0.01	0.67	0.7
^{239}Pu	1,396.2	0.33	0.12	0.01	0.01	0.04	0.4
^{240}Pu	733.4	0.03	0.16	0.13	0.01	0.009	0.2
^{241}Pu	81.5	0.11	0.09	0.64	0.16	0.10	0.7
^{242}Pu	64.2	0.04	0.03	0.03	0.17	0.26	0.3
^{243}Pu	0.0012	3.81	3.26	2.17	3.08	3.78	7.1
^{234}U	1.02	0.03	0.04	0.04	0.02	0.14	0.2
^{235}U	17.2	0.08	0.08	0.07	0.02	0.72	0.7
^{236}U	1.80	0.21	0.15	0.13	0.04	1.13	1.2
^{238}U	11,495.2	0.04	0.01	0.01	0.002	0.01	0.04

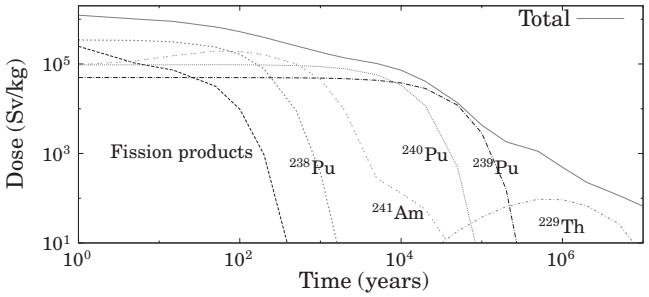

Fig. 10 Radiotoxicity curves for the Kalimer spent fuel up to 10^7 years. Only the main contributors to the total dose are presented in this figure.

correspondent to the last OCTOPUS depletion step. One of the four consecutive core configurations has been selected to study the radiotoxicity. We do not expect significant differences in radiotoxicity between the different core configurations, considering the used semi-random loading strategy. The values provided in this section are for the radiotoxicity of ingestion, calculated using dose coefficients from reports published by ICRP[28] and NRPB.[29]

Following a similar approach, the radiotoxicity curves based on the random calculated spent fuel inventories were calculated. An example of a radiotoxicity curve with the major component is presented in **Fig. 10** up to 10^7 years after irradiation. The evolution of 250 actinides and fission products was followed with FISPACT and their total contribution is presented in **Table 7**, with details for some isotopes in **Tables 8** and **9**.

In the present study, Table 7 shows that the nuclear data used in the transport calculation with MCNP have only a limited impact on the dose calculation (the maximum uncertainty being achieved in a short time after irradiation). Compared with the results presented in Ref. 25) where the uncertainties on the nuclear data used in the inventory code are considered, uncertainties due to transport nuclear data are at least $\simeq 6$ times smaller than the uncertainties due to activation cross sections, depending on the depletion level.

Table 7 Uncertainty due to all considered isotopes (250) for the radiotoxicity dose. Details for different isotope contributions can be found in Tables 8 and 9.

Time (years)	Dose (Sv/kg)	Uncertainty (%) Full correlation (higher limit)	Uncertainty (%) No correlation (lower limit)
1	1.23×10^6	1.0	0.3
5	1.01×10^6	0.8	0.3
15	8.95×10^5	0.8	0.3
50	6.73×10^5	0.8	0.3
100	5.26×10^5	0.7	0.3
200	3.93×10^5	0.7	0.3
500	2.54×10^5	0.6	0.2
10^3	1.84×10^5	0.6	0.2
2×10^3	1.37×10^5	0.5	0.2
5×10^3	1.02×10^5	0.6	0.2
1×10^4	7.28×10^4	0.6	0.2
2×10^4	4.11×10^4	0.6	0.2
5×10^4	1.35×10^4	0.7	0.3
1×10^5	4.29×10^3	0.7	0.4
2×10^5	1.83×10^3	0.8	0.3
5×10^5	1.12×10^3	0.9	0.3
1×10^6	4.91×10^2	0.8	0.3
2×10^6	2.27×10^2	0.7	0.2
5×10^6	1.16×10^2	0.6	0.2

3. Future Work and Improvements for Depletion Calculations

As detailed in the previous sections on the inventory and radiotoxicity, uncertainties due to a part of the nuclear data were obtained. The contribution of the transport nuclear data is nevertheless small and could be neglected in the future if other important uncertainties arise. The current study presents the advantage to assess these uncertainties. The following points can be considered to improve the calculations and to understand the advantages of the TMC method.

- The contribution of the transport and activation nuclear data needs to be addressed at once. Different possibilities can be foreseen, such as modifying OCTOPUS to vary together the nuclear data for MCNP and for FISPACT. Another solution would be to use a simulation code where the distinction between transport and activation nuclear data libraries is not artificially made, such as the integrated transport and depletion Monte Carlo code SERPENT.[30)]
- As presented above, the correlation between isotopes is important if standard reactions are included in the study. This issue cannot be ignored in any use of nuclear data and nuclear data uncertainties related to a large number of nuclei. The existing nuclear data libraries (well recognized such as ENDF/B-VII.0[31)] or under development such as the TENDL series[32,33)]) do not include (or very barely) the cross correlation between isotopes. In the case of the TMC method, as no covariance files are used, it seems at first difficult to include the cross correlation

Table 8 Uncertainty due to isotopes presented in Table 7 for the radiotoxicity dose (lower limit, with no correlation for the nuclear data)

Time (years)	Dose (kSv/kg) ^{90}Sr	^{134}Cs	^{137}Cs	^{238}Pu	^{239}Pu	^{240}Pu	^{241}Pu	^{241}Am	^{244}Cm
1	54.08 ± 0.03	23.78 ± 0.42	46.37 ± 0.03	344.1 ± 0.3	49.70 ± 0.21	95.59 ± 0.23	88.27 ± 0.70	96.14 ± 0.25	254.0 ± 2.1
5	49.13 ± 0.02	6.21 ± 0.11	42.30 ± 0.03	337.2 ± 0.3	49.69 ± 0.21	95.75 ± 0.23	72.81 ± 0.58	116.9 ± 0.32	217.9 ± 1.8
15	38.63 ± 0.02	0.22 ± 0.00	33.61 ± 0.02	312.6 ± 0.2	49.68 ± 0.21	96.05 ± 0.23	45.00 ± 0.36	153.3 ± 0.56	148.6 ± 1.2
50	16.67 ± 0.01	—	15.04 ± 0.01	239.7 ± 0.2	49.63 ± 0.21	96.33 ± 0.23	8.35 ± 0.07	194.0 ± 0.90	38.90 ± 0.32
100	5.02 ± 0.00	—	4.77 ± 0.00	164.4 ± 0.1	49.57 ± 0.21	96.01 ± 0.23	0.76 ± 0.01	189.0 ± 0.90	5.73 ± 0.47
200	0.45 ± 0.00	—	0.48 ± 0.00	78.11 ± 0.05	49.43 ± 0.21	95.03 ± 0.23	—	162.0 ± 0.78	0.12 ± 0.00
500	—	—	—	9.07 ± 0.01	49.03 ± 0.21	92.07 ± 0.22	—	100.3 ± 0.48	—
10^3	—	—	—	0.37 ± 0.00	48.35 ± 0.21	87.33 ± 0.19	—	45.16 ± 0.21	—
2×10^3	—	—	—	—	47.04 ± 0.20	78.58 ± 0.16	—	9.29 ± 0.00	—
5×10^3	—	—	—	—	43.28 ± 0.18	57.24 ± 0.14	—	0.27 ± 0.00	—
1×10^4	—	—	—	—	37.63 ± 0.16	33.76 ± 0.08	—	—	—
2×10^4	—	—	—	—	28.36 ± 0.12	11.74 ± 0.03	—	—	—
5×10^4	—	—	—	—	12.02 ± 0.05	0.49 ± 0.00	—	—	—
1×10^5	—	—	—	—	2.85 ± 0.01	—	—	—	—
2×10^5	—	—	—	—	0.16 ± 0.00	—	—	—	—
5×10^5	—	—	—	—	—	—	—	—	—
1×10^6	—	—	—	—	—	—	—	—	—
2×10^6	—	—	—	—	—	—	—	—	—
5×10^6	—	—	—	—	—	—	—	—	—

Table 9 Uncertainty due to isotopes presented in Table 7 for the radiotoxicity dose (lower limit, with no correlation for the nuclear data)

Time (years)	Dose (Sv/kg)							
	^{85}Kr	^{106}Ru	^{125}Sb	^{147}Pm	^{210}Po	^{222}Rn	^{243}Am	^{243}Cm
1	240.1 ± 0.4	$61{,}523 \pm 66$	381.2 ± 0.5	$1{,}991 \pm 5$	—	—	$1{,}719 \pm 8$	$2{,}953 \pm 322$
5	185.4 ± 0.3	$3{,}931 \pm 4$	139.5 ± 0.2	691.6 ± 2	—	—	$1{,}718 \pm 8$	$2{,}692 \pm 294$
15	97.2 ± 0.1	4.0 ± 0.0	11.3 ± 0.0	49.2 ± 0.1	—	—	$1{,}717 \pm 8$	$2{,}137 \pm 233$
50	10.1 ± 0.0	—	—	—	—	—	$1{,}711 \pm 8$	952.0 ± 104
100	—	—	—	—	—	—	$1{,}703 \pm 8$	299.8 ± 32
200	—	—	—	—	—	—	$1{,}687 \pm 8$	29.7 ± 3.2
500	—	—	—	—	—	—	$1{,}640 \pm 8$	—
10^3	—	—	—	—	—	—	$1{,}564 \pm 8$	—
2×10^3	—	—	—	—	3.7 ± 0.0	22.6 ± 0.0	$1{,}424 \pm 8$	—
5×10^3	—	—	—	—	17.9 ± 0.0	58.9 ± 0.0	$1{,}073 \pm 8$	—
1×10^4	—	—	—	—	47.0 ± 0.0	128.8 ± 0.4	670.8 ± 3	—
2×10^4	—	—	—	—	102.7 ± 0.7	292.9 ± 0.9	261.7 ± 1.2	—
5×10^4	—	—	—	—	233.8 ± 1.6	451.2 ± 3.1	15.5 ± 0.1	—
1×10^5	—	—	—	—	360.6 ± 2.5	528.4 ± 3.6	—	—
2×10^5	—	—	—	—	422.7 ± 2.9	315.0 ± 2.1	—	—
5×10^5	—	—	—	—	252.9 ± 1.7	90.4 ± 0.5	—	—
1×10^6	—	—	—	—	72.8 ± 0.4	18.3 ± 0.0	—	—
2×10^6	—	—	—	—	—	—	—	—
5×10^6	—	—	—	—	—	—	—	—

between isotopes. There is one inherent cross correlation due to the use of the TALYS code, which introduces a theoretical cross correlation for all nuclei, but this cross correlation does not correspond to the experimental usage of standard cross sections. A possible solution would be to create a cross correlation between a standard (such as ^{238}U) and another nucleus (such as ^{241}Am) by using the same sequence of random numbers for the generation of random nuclear parameters for the TALYS inputs. This artificial cross correlation through random numbers would simulate the experimental cross correlation: if the same random numbers are used to obtain for instance the height of a fission barrier, a similar behavior will be obtained for both fission cross sections, implying strong cross correlations.

- The other important source of nuclear data uncertainties in calculations with inventory codes is the decay data. Generally not considered, decay data might have a large impact, for instance, by varying the half-life or decay probability of some nuclei. Up to now, there are no covariance files for decay data, except that the decay data library includes uncertainties on some quantities, such as half-life and normalization of spectra. Bypassing the use of covariance files, the TMC method can be used to produce random decay data libraries, fission yields, and to perform random depletion calculations.

It should be emphasized again that one of the large advantages of the TMC method compared with other methods is that all types of transport nuclear data are considered: not only cross sections, but also angular distribution, neutron emission, energy of the emitted particles, and so on. If the TMC method is applied with activation or decay nuclear data, a similar statement can be made about all types of decay quantities.

VI. Conclusions

In this study, the impact of nuclear data used in the transport calculation has been evaluated for different parameters of the KALIMER Sodium Fast Reactor with the Total Monte Carlo and perturbation methods. Transport simulations were carried out with the MCNP code and inventory calculations were performed with FISPACT. Uncertainties due to the transport nuclear data were propagated to k_{eff}, β_{eff}, the sodium void reactivity coefficient, and the fuel inventory at the end of cycle with radiotoxicity curves up to 10^7 years. The impact on k_{eff}, β_{eff}, and the sodium void reactivity coefficient is not negligible, and the current knowledge on nuclear data seems to be inadequate to meet the target accuracy for such reactors (for the void reactivity coefficient, a target accuracy of 4% is required, and sodium nuclear data only contributes to 6%). Concerning the fuel inventory and radiotoxicity, the impact of transport nuclear data is rather limited. In this case, other sources of uncertainties might be more meaningful, such as activation cross sections and decay data (for depletion calculation). As future work, we plan to study the effect of activation, decay data, and fission yield covariances on a similar reactor type. The Total Monte Carlo will probably be the most flexible for this purpose.

References

1) T. Sugawara, K. Nishihara, K. Tsujimoto, T. Sasa, H. Oigawa, "Analytical validation of uncertainty in reactor physics parameters for nuclear transmutation systems," *J. Nucl. Sci. Technol.*, **47**, 521 (2010).
2) G. Pandikumar, V. Gopalakrishnan, P. Mohanakrishnan, "Impact of spread in minor actinide data from ENDF/B-VII.0, ENDF/B-VI.8, JENDL-3.3 and JEFF-3.0 on an IAEA-CRP FBR benchmark for MA incineration," *Ann. Nucl. Energy*, **35**,

1519 (2008).
3) D. Rochman, A. J. Koning, D. F. da Cruz, P. Archier, J. Tommasi, "On the evaluation of ^{23}Na neutron-induced reactions and validations," *Nucl. Instrum. Methods*, **A612**, 374 (2010).
4) A. J. Koning, D. Rochman, "Towards sustainable nuclear energy: Putting nuclear physics to work," *Ann. Nucl. Energy*, **35**, 2024 (2008).
5) D. Rochman, A. J. Koning, S. C. van der Marck, "Uncertainties for criticality-safety benchmarks and k_{eff} distributions," *Ann. Nucl. Energy*, **36**, 810 (2009).
6) D. Rochman, A. J. Koning, S. C. van der Marck, "Exact nuclear data uncertainty propagation for fusion neutronics calculations," *Fusion Eng. Des.*, **85**, 669 (2010).
7) D. Hahn, Y.-I. Kim, C. B. Lee, S.-O. Kim, J.-H. Lee, Y.-Y. Lee, B.-H. Kim, H.-Y. Jeong, "Conceptual design of the sodium-cooled fast reactor KALIMER-600," *Nucl. Eng. Technol.*, **39**, 193 (2007).
8) S. G. Hong, S. J. Kim, H. Song, Y.-I. Kim, "Neutronic design of KALIMER-600 core with moderator rods," *Proc. ICAPP'04: 2004 International Congress on Advances in Nuclear Power Plants*, Pittsburgh, USA, Jun. 13–17, 2004, 646 (2004).
9) D. Hahn, private communication (2009).
10) J. F. Briesmeister (Ed.), *MCNP—A General Monte Carlo Code n-Particle Transport Code*, version 4C, Report LA-13709-M, Los Alamos National Laboratory (2000).
11) A. Hogenbirk, "An easy way to carry out 3D uncertainty analysis," *Proc. Joint Int. Top. Mtg. on Mathematics and Computation and Supercomputing in Nuclear Applications (M&C+SNA 2007)*, Monterey, California, USA, Apr. 15–19, 2007 (2007), [CD-ROM].
12) R. McFarlane, D. W. Miur, *The NJOY Nuclear Data Processing System, Version 91*, LA-17740-M, Los Alamos National Laboratory (1994).
13) K. Furuta, Y. Oka, S. Kondo, *SUSD: A Computer Code for Cross Section Sensitivity and Uncertainty Analysis Including Secondary Neutron Energy and Angular Distributions*, UTNL-R0185, Nucl. Eng. Res. Lab, University of Tokyo (1986).
14) D. Rochman, A. J. Koning, S. C. van der Marck, A. Hogenbirk, C. Sciolla, "Nuclear data uncertainty propagation: Monte Carlo vs. perturbation," *Ann. Nucl. Energy*, **38**, 942 (2011).
15) D. Rochman, A. J. Koning, *TENDL-2010: TENDL-2010: Reaching Completeness and Accuracy*, OECD/NEA JEF/DOC-1349, http://www.talys.eu/tendl-2010 (2010).
16) Working Party on International Evaluation Co-operation of the NEA Nuclear Science Committee, *Uncertainty and Target Accuracy Assessment for Innovative Systems Using Recent Covariance Data Evaluations*, OECD, Volume 26, 78 (2008).
17) A. J. Koning, S. Hilaire, M. C. Duijvestijn, "TALYS-1.0," *Proc. Int. Conf. on Nuclear Data for Science and Technology—ND2007*, Nice, France, May 22–27, 2007 (2007).
18) D. Rochman, A. J. Koning, S. C. van der Marck, A. Hogenbirk, D. van Veen, "Nuclear data uncertainty propagation: Total Monte Carlo vs. covariances," *Proc. Int. Conf. on Nuclear Data for Science and Technology, ND2010*, Jeju, Korea, Apr. 26–30, 2010 (2010).
19) R. K. Meulekamp, S. C. van der Marck, "Calculating the effective delayed neutron fraction with Monte Carlo," *Nucl. Sci. Eng.*, **152**, 142 (2006).
20) R. Capote, D. L. Smith, "An investigation of the performance of the unified Monte Carlo method of neutron cross section data evaluation," *Nucl. Data Sheets*, **109**, 2768 (2008).
21) J. A. Favorite, "Eigenvalue sensitivity analysis using the MCNP5 perturbation capability," *Proc. Mtg. of the ANS Nuclear Criticality Safety Division, NCSD-2009*, Richland, Washington, USA, Sept. 13–17, 2009 (2009).
22) B. T. Rearden, D. E. Peplow, "Comparison of sensitivity analysis techniques in Monte Carlo codes for multi-region criticality calculations," *Trans. Am. Nucl. Soc.*, **85**, 163 (2001).
23) J. A. Favorite, "An alternative implementation of the differential operator (Taylor series) perturbation method for Monte Carlo criticality problems," *Nucl. Sci. Eng.*, **142**, 327 (2002).
24) B. T. Rearden, *TSUNAMI-3D: Control Module for Three-Dimensional Cross-Section Sensitivity and Uncertainty Analysis for Criticality*, ORNL/TM-2005/39 Version 6, Vol. I, Sect. C9, Oak Ridge National Laboratory (2009).
25) N. Garcìa-Herranz, O. Cabellos, F. Àlvarez-Velarde, J. Sanz, E. M. Gonzàlez-Romero, J. Juan, "Nuclear data requirements for the ADS conceptual design EFIT: Uncertainty and sensitivity study," *Ann. Nucl. Energy*, **37**, 1570 (2011).
26) J. Oppe, J. C. Kuijper, *OCTOPUS_TNG Reference Guide*, NRG Report 20748/03.54103/C, the Netherlands (2004).
27) R. A. Forrest, *The European Activation System: EASY-2001 Overview*, UKAEA FUS 449, United Kingdom (2001).
28) International Commission of Radiological Protection, *Dose Coefficients for Intakes of Radionuclides by Workers*, ICRP Publication 68, Pergamon Press, Oxford (1995); *Age-Dependent Doses to Members of the Public from Intake of Radionuclides: Part 5*, ICRP Publication 72, Pergamon Press, Oxford (1996).
29) A. W. Philips, G. M. Kendall, J. W. Stather, T. P. Fell, *Committed Equivalent Organ Doses and Committed Effective Doses from Intakes of Radionuclides*, NRPB-R245 (1991); A. W. Philipps, T. J. Silk, *Dosimetric Data for Fusion Applications*, NRPB-M589 (1995).
30) J. Leppänen, "PSG2/Serpent, a Continuous-energy Monte Carlo reactor physics burnup calculation code," VTT Technical Research Centre of Finland, http://montecarlo.vtt.fi (2010).
31) M. B. Chadwick *et al.*, "ENDF/B-VII.0: Next generation evaluated nuclear data library for nuclear science and technology," *Nuclear Data Sheets*, **107**, 2931 (2006).
32) A. J. Koning, D. Rochman, *TENDL-2008: Consistent Talys-Based Evaluated Nuclear Data Library Including Covariances*, OECD/NEA JEF/DOC-1262, http://www.talys.eu/tendl-2008 (2008).
33) A. J. Koning, D. Rochman, *TENDL-2009: Consistent Talys-Based Evaluated Nuclear Data Library Including Covariances*, OECD/NEA JEF/DOC-1310, http://www.talys.eu/tendl-2009 (2009).